Accepted Manuscript

Enabling Low Power Acoustics for Capillary Sonoreactors

Francisco J. Navarro-Brull, Andrew R. Teixeira, Gaurav Giri, Roberto Gómez

PII: S1350-4177(18)31810-8
DOI: https://doi.org/10.1016/j.ultsonch.2019.03.013
Reference: ULTSON 4522

To appear in: *Ultrasonics Sonochemistry*

Received Date: 7 December 2018
Revised Date: 8 March 2019
Accepted Date: 12 March 2019

Please cite this article as: F.J. Navarro-Brull, A.R. Teixeira, G. Giri, R. Gómez, Enabling Low Power Acoustics for Capillary Sonoreactors, *Ultrasonics Sonochemistry* (2019), doi: https://doi.org/10.1016/j.ultsonch.2019.03.013

Enabling Low Power Acoustics for Capillary Sonoreactors

Francisco J. Navarro-Brull[1], Andrew R. Teixeira[2], Gaurav Giri[3], Roberto Gómez[1,*]

[1]*Institut Universitari d'Electroquímica i Departament de Química Física, Universitat d'Alacant, Apartat 99, E-03080, Alicante, Spain*

[2]*Department of Chemical Engineering, Worcester Polytechnic Institute, Worcester, MA 01609, United States*

[3]*Department of Chemical Engineering, University of Virginia, Charlottesville, Virginia 22904, United States*

*Corresponding author. E-mail address: roberto.gomez@ua.es (R. Gómez)

Abstract:

Capillary reactors demonstrate outstanding potential for on-demand flow chemistry applications. However, non-uniform distribution of multiphase flows, poor solid handling, and the risk of clogging limit their usability for continuous manufacturing. While ultrasonic irradiation has been traditionally applied to address some of these limitations, their acoustic efficiency, uniformity and scalability to larger reactor systems are often disregarded. In this work, high-speed microscopic imaging reveals how cavitation-free ultrasound can unclog and prevent the blockage of capillary reactors. Modeling techniques are then adapted from traditional acoustic designs and applied to simulate and prototype sonoreactors with wider and more uniform sonication areas. Blade-, block- and cylindrical shape sonotrodes were optimized to accommodate longer capillary lengths in sonoreactors resonating at 28 kHz. Finally, a novel helicoidal capillary sonoreactor is proposed to potentially deal with a high concentration of solid particles in miniaturized flow chemistry. The acoustic designs and first principle rationalization presented here offer a transformative step forward in the scale-up of efficient capillary sonoreactors.

Keywords: Power ultrasound, capillary sonoreactor, clogging, scale-up, modeling, microreactors

Introduction

Capillary reactors can exhibit practical advantages over microreactors as they allow higher throughput and better solid management [1,2]. By increasing the diameter of the reactor to millimeters instead of tens/hundreds of micrometers, the high surface area-to-volume ratio of milli-scale reactors is still able to achieve reactions under controlled conditions and enhanced heat and mass transfer rates. Examples of the versatility afforded by commercial capillary tubing and fittings instead of lab-on-a-chip devices have recently been published for fine chemistry in the pharmaceutical sciences [3]. Yet, the handling of solids (catalysts, reagents, precipitation of products or by-products) is still one of the main drawbacks limiting their operating window [4–7]. During a reaction, the formation of solid aggregates or precipitates can irreversibly clog the capillary tubing or connectors, leading to delays in production and increased shut down/startup costs [6].

The use of ultrasonic irradiation has been successfully implemented not only to prevent clogging but also to enhance mass transport in multiphase flow through cavitation [4,8–18]. Traditionally, the immersion of capillaries in ultrasonic baths [19], the integration of miniaturized piezoelectric transducers [8,20], or the placement of ultrasonic horns in the proximity of reacting tubes [21], have been used for this purpose, among others [12]. The generated acoustic field strongly depends on how the entire device resonates, a phenomenon well studied in the area of microfluidics defined as acoustofluidics [22–24]. Acoustic forces —including streaming— can be focused on the center of capillaries, minimizing the risk of clogging as recently shown in microreactor systems [25]. For capillary sonoreactors on a larger scale, the applied frequency can either be adjusted once the device is mounted [8], or rationalized via the construction materials, sizes and geometries [26]. Analytical approaches using the Langevin equation or electromechanical equivalent circuits [27–30] can be a good starting point for the design of sonoreactors.

Although ultrasound is usually found to improve solid handling [21] during the production of active pharmaceutical ingredients [7,31], the scaled-up application of high power ultrasound to longer capillary length is still challenging [32–35] as the main vibrational modes cause the appearance of nodes and antinodes across the sonicated area. In fact, a major limitation preventing full exploitation of scaled-up sonoreactors is the lack of a proper methodology to avoid a numbering up strategy or the use of ultrasonic baths when longer capillary reactors lengths are needed.

In any case, it is worth emphasizing that acoustic irradiation is an active method to handle solids and avoid clogging in continuous-flow capillary systems [4,5,36], typically applied in the

form of ultrasonic baths [37]. The main clogging mechanisms in capillary reactors usually involve bridging, fouling or particle deposition [6,9,38]. The usage of power ultrasound to prevent or remediate the blockage of capillary sonoreactors has been often related to cavitation [8,10], as it is the case in ultrasonic cleaning applications [39–44]. However, recent acoustic applications to micropacked-bed reactors [45] indicate that additional mechanisms can produce partial particle fluidization. For instance, purely vibratory forces have been traditionally applied to avoid the formation of jams in hoppers or silos [46–48]. Recent understanding of the physics of granular materials such as arch or bridge formation [49,50] and particle stress distributions [51,52] favors the use of internal or external energy sources that can be reapplied to different scales of interest [48].

In this work, we use scalable acoustic design principles to obtain highly focused, wider and more uniform sonication areas. The unclogging mechanism in capillary tubing is captured first using low-power ultrasound and high-speed optical imaging. Advanced numerical methods are then used to optimize a diverse variety of sonoreactor designs. A proper understanding of the vibrational modes leads to a novel helicoidal capillary sonoreactor.

Materials and methods

Acoustic Design, Modeling and Optimization of Sonoreactors

High-power ultrasonic devices are widely used in manufacturing industries [53–57] and usually consist of an ultrasonic transducer attached to a probe, sonotrode or horn, which acts as a waveguide (see **Figure 1**). The design of ultrasonic devices maximizes their vibrational modes in one direction and at a specific resonant frequency [27,58,59], [60,61], generally along their axis of symmetry.

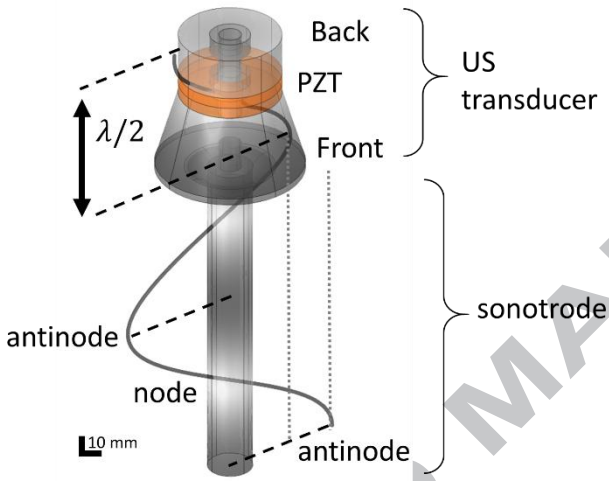

Figure 1. Common elements within high-power ultrasonic devices designed as a function of the wavelength λ [m], which corresponds to the ratio between the speed of sound (*c* [m/s]) and the applied frequency (*f* [Hz]). The total displacement —shown in grayscale and as a waveform— is mainly longitudinal with a maximum (antinode) at the tip of the sonotrode.

The driving frequency selection and use of sonotrodes are thus tailored to the intensity required in each application [62]. Different sonotrode geometries can modify the ultrasonic vibrational modes due to changes in the speeds at which the deformations are propagated through the solid material and the different distribution of masses [63]. In this regard, the performance of the sonotrodes is predicted in a more straightforward way when the acoustic propagation is physically confined —e.g. lateral or perpendicular dimensions below a third of the wavelength (see **Figure S1**) —. When wider sonication areas are necessary, slits confining the vibrations in one direction are a standard feature in commercial sonotrodes. By following this design approach, analytical expressions can be derived for the initial design of wide-area resonant structures [64,65]. Yet, the sizing and location of a capillary reactor with a commercial transducer and sonotrode is not trivial. If it is placed without adequate consideration, the resonant frequency and vibrational mode of the assembled system can be significantly modified

from the desired specifications [66]. The appearance of nodes and antinodes at distinct locations will cause spatially-resolved areas of low-acoustic performance and structural failures due to fatigue. Therefore, a modeling and simulation approach becomes crucial to optimize the performance of wide-area sonoreactors during prototyping stages.

Simulation strategies that capture the physics of interest are well known from the literature [67–74]. Our approach focuses on the design of evenly-distributed and wide-sonicating areas when prototyping acoustically-enhanced capillary reactors. To this end, a commercial Finite Element Method (FEM) software (COMSOL Multiphysics v.4.4, AB) is used in this work to discretize and numerically solve the equations described in the Supplementary Material. Isotropic energy losses and attenuation factors are included in the description of the model and only relative values of displacements and acoustic pressures are provided, which are assumed to be proportional to the low voltage applied to the piezos [66,75–77]. The validation of the modeling and simulation approach used in this paper, presented at the beginning of the results section, thus focuses on comparing the predicted and experimentally observed vibrational modes. More sophisticated models would be necessary to capture phenomena such as non-linear attenuation in cavitating liquids [78,79] and acoustic streaming in the presence of cavitation [80].

Experimental methods

An ultrasonic power generator (Undatim Ultrasonics SA, BE) was used to find the resonant frequencies and validate the simulation results. The capillary sonoreactor parameters used for validation were fixed in both cases to 100 mm and 3.17 mm of length and internal diameter, respectively. The versatility of this geometry has been proven in the literature and it is widely studied as a micropacked-bed reactor [81,82]. To reduce the stress concentration, the outer reactor diameter was chosen to be 12.7 mm. Stainless steel (316L) was used due to its better chemical compatibility when compared to other commonly-used sonotrode materials, such as aluminum or titanium. To ease the prototyping and reduce manufacturing costs, a 28 kHz commercial high-power ultrasonic transducer (APC International, Ltd. USA) was used. The sonotrode designs were machined and tightly bolted to the ultrasonic transducer. Commercial drill bits (BM12x230 and BM12x460 Celesa Bluemaster, Spain) were used for prototyping the helicoidal sonoreactors. Given the geometry, material properties, and frequency of interest, the initial sonotrode dimensions were obtained by respecting the distances imposed by the longitudinal wavelength. Then, the resonant structures were acoustically optimized following the strategy described in the Supplementary Material.

The vibrational modes were also captured experimentally by placing 250 μm silica beads on the surface of the sonotrode, particle motion induced by vibrations was recorded using a high-speed camera. A time-resolved particle image velocimetry software [83] was used to obtain the experimental displacement field.

A simplified setup was used to visualize the clogging and unclogging mechanism at high speed when ultrasound was applied. A HARVARD PhD Ultra syringe pump was connected to a series of stainless steel Swagelok manual valves and 1/8" PFA IDEX Health & Science tubing. The system allowed the introduction of 90-150 μm KCl crystals into the feeding line to promote the clogging downstream. A saturated KCl solution with the high concentration of suspended crystals passed through a reducing union (Vici Valco Instrument Co, ZRU21 316 stainless steel), which was sonicated with an external 40 kHz ultrasonic cleaning transducer (APC International Ltd, APC-90-4050). Downstream the tubing (1/16" PFA IDEX Health & Science) was thermally treated to reduce its ID from 1.09 mm to a 0.63 mm. At this point, an inverted microscope (Carl Zeiss) and a high-speed camera (Phantom™ Vision Research) were used to capture the clogging as well as the unclogging mechanisms. The probe of a miniaturized ultrasonic cleaning transducer (APC International Ltd, APC-4SS-1550) was used to sonicate the clog on demand by means of a function generator (Siglent SDG1025) with an amplifier (E&I 1020L). The minimum power supplied by this setup was used, with a signal output of 2 mVpp at 51 kHz, consuming 1 W of load power. The A custom-machined microscope plate compressed the tubing between a set screw and the miniaturized ultrasonic device. Additional experiments were made using such a compression system to promote clogging.

Results and discussion:

High-speed microscopic imaging can be used to understand how ultrasonic irradiation at low frequencies (51 kHz) promotes the local fluidization of a clog formed by ~90-150 μm KCl crystals (**Figure 2)**. Low-power sonication (1W) can prevent and avoid clog formation even when there is a sudden reduction of capillary cross-sectional area (**Figure 2a**). This proof-of-concept visualization illustrates the importance that vibrations spread over areas where clogging can occur, rather than providing high-amplitude local ultrasonication to induce cavitation. It is worth noting that no cavitation was experimentally observed under the conditions used in this work (see supplementary videos).

Different scale-up strategies and designs of capillary sonoreactors will be described to achieve the specific goal of distributed low power acoustics in capillary reactors. The design of a miniaturized sonoreactor is first evaluated by considering two basic configurations: a longitudinal- and a perpendicular-wise design. To increase the sonicated area and accommodate longer reactor lengths, sonotrodes including a blade-, block- and cylindrical-like geometries, are acoustically designed using both analytical and numerical approaches. A novel acoustic design using a helicoidal sonotrode is then proposed and characterized at the end of this section.

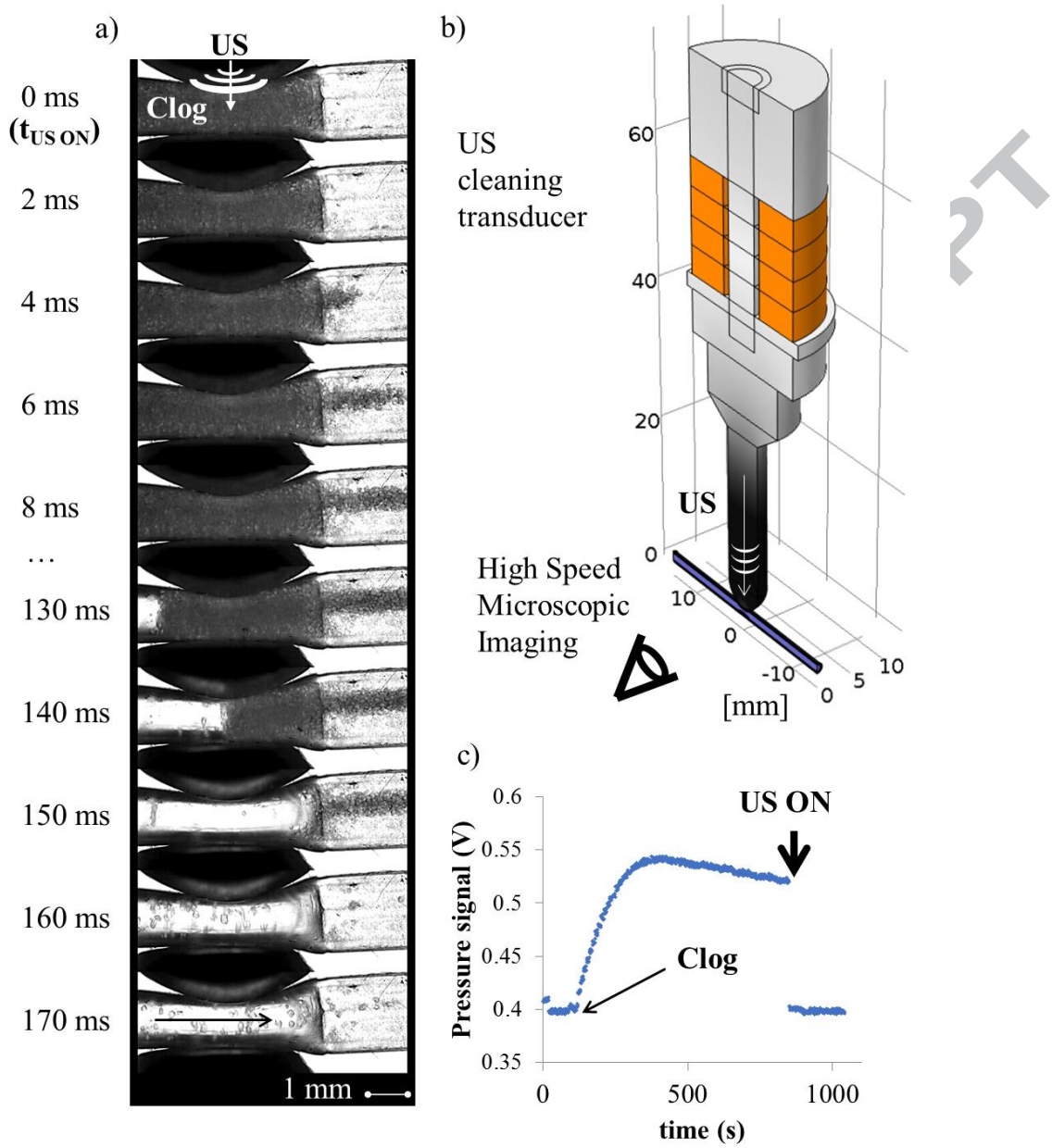

Figure 2. Imaging of clogging and ultrasonic unclogging events (a) in a controlled geometry restriction (1.09 mm ID reduced to 0.63 mm over 6 mm of length). The sonication system (b) is located at the capillary restriction. c) Pressure drop signal was monitored during the experiments (1 ml/min of KCl-saturated water, 51 kHz and 1 W of power). High speed video visualizations showing the ultrasonic fluidization of 90-150 µm KCl are included as supplementary material.

Longitudinal and perpendicular sonoreactors

Langevin or sandwich transducers are usually designed to maximize the displacement along its longitudinal direction. Thus, to efficiently sonicate reduced reactor lengths, two main options can be examined, namely, an axisymmetric longitudinal design or a perpendicular configuration (**Figure 3 and 4**, respectively).

As intended, the numerically resolved prototypes resonated close to the 28 kHz natural frequency of the ultrasonic transducer they were designed for. The longitudinal design (**Figure 3**) was machined from a 70 mm diameter cylindrical block. The axisymmetric unibody design allowed an accurate prediction by the model with only a slight difference of ~0.1 kHz when compared to the experimentally observed resonance. The perpendicular configuration showed ~1 kHz difference with respect to the model, probably due to the soldering of a 12.7 mm diameter stainless-steel tubing instead of machining the sonotrode from one piece. The assembled sonoreactors were not acoustically adjusted by removing material as is usually the case in manufacturing industries. At their resonant frequency, nodal points exactly matched those predicted in the simulations (see **Figure 3b and 4c**).

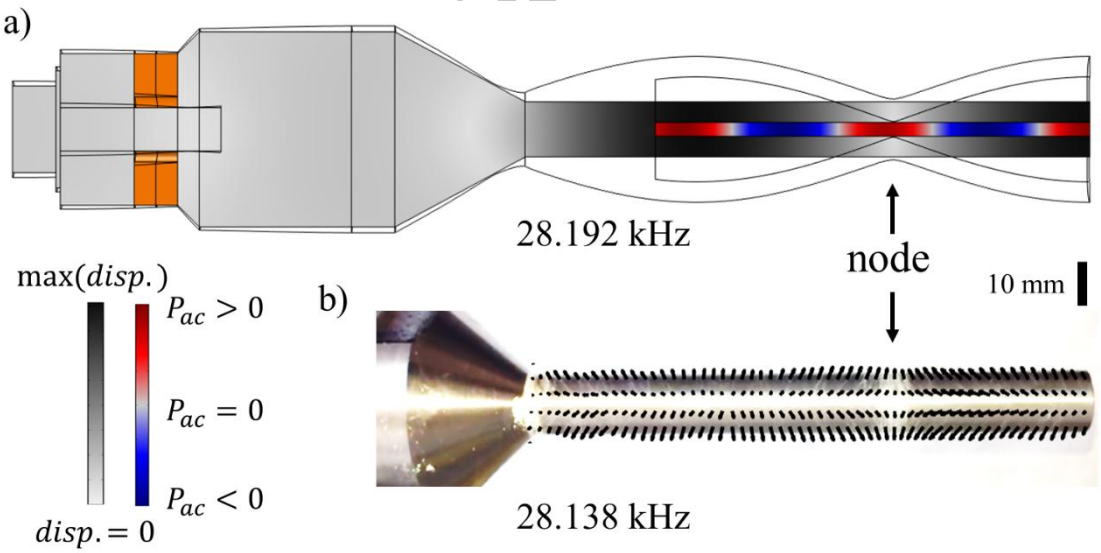

Figure 3. Longitudinal design where the reactor chamber is located within the sonotrode, following its axisymmetry. The predicted displacements (a, grey scale) were validated by tracking the motion response of particles at the surface (b). The resonant frequency of the model (a) and the assembled prototype (b) were 28.192 and 28.138 kHz, respectively. The acoustic pressure (red to blue color scale) is calculated assuming a lossless media.

The benefits of using longitudinal sonotrodes are several, in theory: they are the simplest to manufacture and the selected funnel shape (truncated cone plus cylindrical reactor) has a well-known analytical expression that can be used to obtain the initial dimensions [64]. The stress concentration was minimized by locating the notch of the sonotrode at a nodal point (**Figure 3**). Gaussian belled, exponential or catenoidal longitudinal cross-section reductions can also be used to further reduce long-term fatigue failures and provide higher mechanical amplifications [65]. Longitudinal designs allow screwed fittings at the areas where the displacement is maximized (antinodes) avoiding clogging issues when dealing with solids. However, the acoustic pressure distribution, as well as displacements, seems to be determined by the wavelength of the media (standing waves can be identified as a longitudinal pattern in 3a).

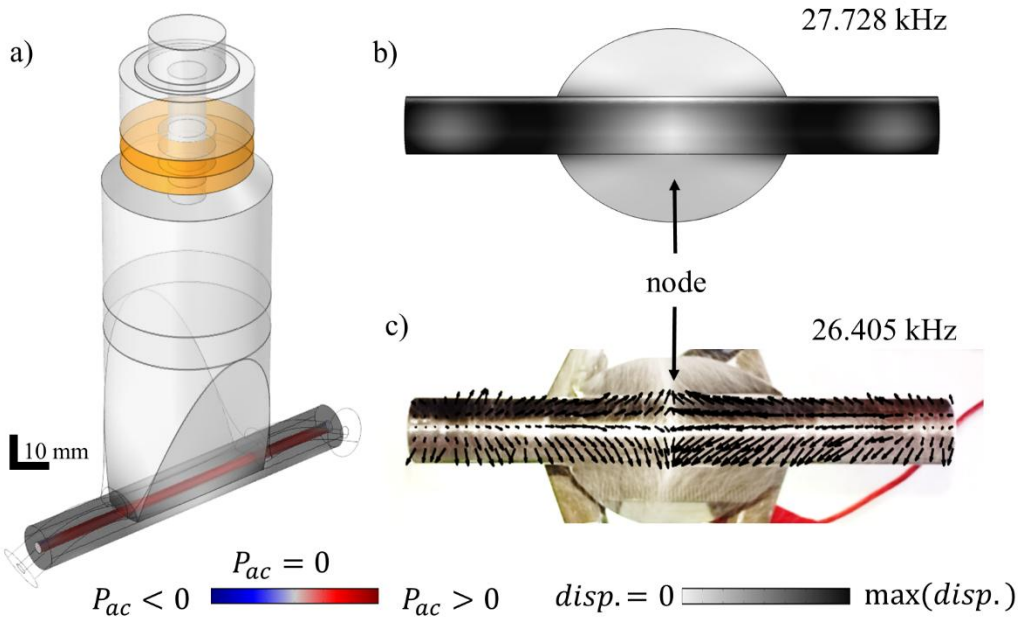

Figure 4. Perpendicular sonotrode design (a) where the reactor chamber receives the mechanic vibrations normal to the longitudinal motion created by the ultrasonic transducer. The theoretical magnitude of the displacement and the experimentally tracked motion are shown in b and c (grey scale and arrow field, respectively). The model results are validated against the particle motion at the bottom of the sonotrode.

When the reactor chamber is placed at an antinode, but perpendicular to its longitudinal axis (**Figure 4a**), the acoustic pressure is better distributed. The vibrational mode also affects the pressure that can be achieved. In this case, a nodal point appears at the center of the tube, captured both in the model and in the experimental validation as seen in **Figure 4b and 4c**, respectively.

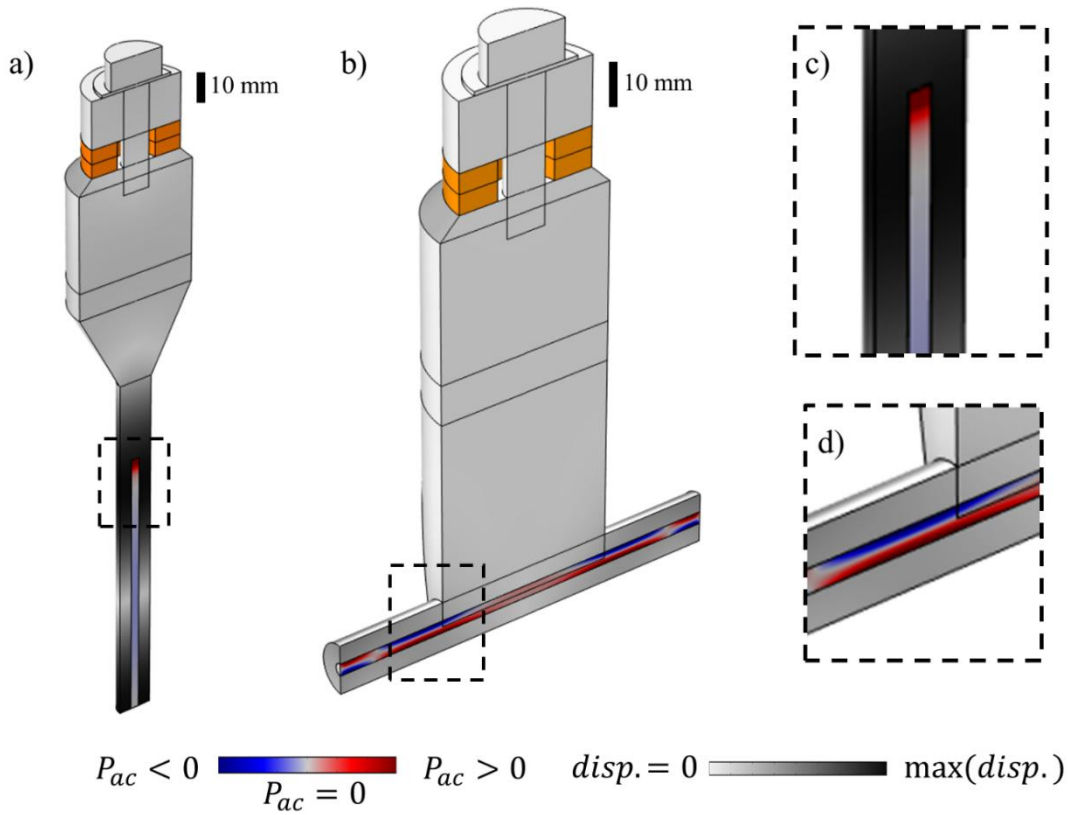

Figure 5. Sonotrode configurations (a longitudinal and b perpendicular) with attenuation included in the modeled liquid medium. The acoustic pressure decreases quickly in the longitudinal design (c). The perpendicular design shows better distribution (d) thanks to its larger surface area normal to the main longitudinal vibrations created by the ultrasonic transducer.

The advantage of perpendicular sonotrode geometries compared to the longitudinal ones can be better deduced from **Figure 5.** Damping is likely to occur in viscous, porous or liquid media that experience cavitation. If severe attenuation is present in the reactant medium, the mechanical energy will be mainly transmitted close to the antinodes corresponding to vibrational modes normal to the reactor walls. When scaling up, the goal is to achieve well focused and uniform displacements at the inner channel walls. This will ensure agitation at the phase interface where clogging is most likely and enable the propagation of acoustic energy into the fluid phase. Therefore, an optimal design will not have areas of severe nodal points, spikes or dips in either metric.

Scale-up of capillary sonoreactors

When designing ultrasonic devices, the appearance of nodes and antinodes at the vibrating surface is limited, in theory, by the frequency applied and the resonant mode of the sonotrode [34,35]. To increase the sonicated area, blade-, block- and cylindrical-like sonotrodes are commonly found in the ultrasonic industry [53,62,64,84–86]. These are highly optimized devices that evenly distribute the displacement via slits and additional masses. Analytical and numerical approaches [64,65] were used to obtain the initial design parameters to optimize capillary sonoreactors.

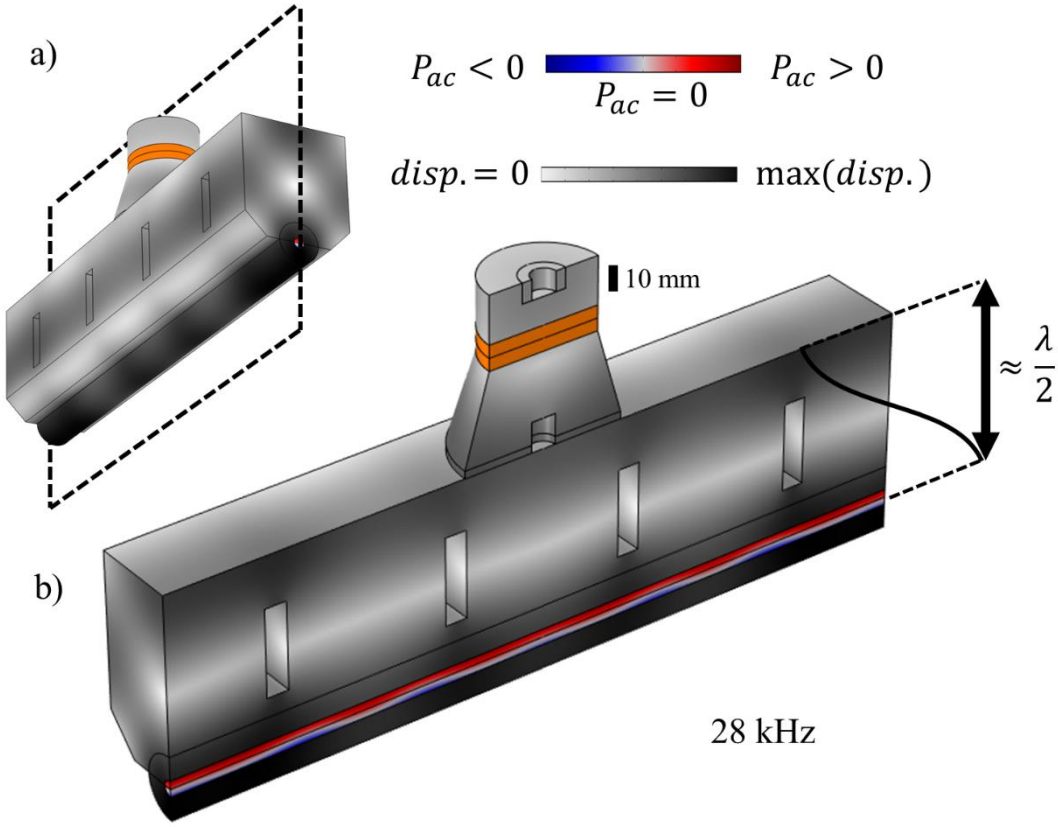

Figure 6. Blade-type sonotrode with four slits (a) to increase the sonicated surface area while maintaining a distributed displacement field (colored) designed for a 28 kHz ultrasonic transducer. A reduction in the cross-section area at the end of the sonotrode maximizes the vibration amplitude for single reactors as seen in the cross-sectional view (b).

A wider sonotrode with four slits made of aluminum was dimensioned for a 28 kHz ultrasonic transducer (**Figure 6**). Commonly known as blade sonotrodes [65], this configuration is used in the cutting industry and benefits from the increase in amplitude given by the reduction of cross-sectional area at the tip of the sonotrode. When a capillary reactor (**Figure 6b**) is placed

at the tip, the slits homogenize the distribution of the displacements and acoustic field. The main benefit is the capability of increasing the sonicated length of the capillary reactor when compared with the simpler transversal prototype shown in **Figure 4**. Reactor dimensions and vibration frequency were maintained at the same parameters to allow the comparison of the two approaches. Wider reactor diameters are also possible if the dampening in the media is not too severe [87–90].

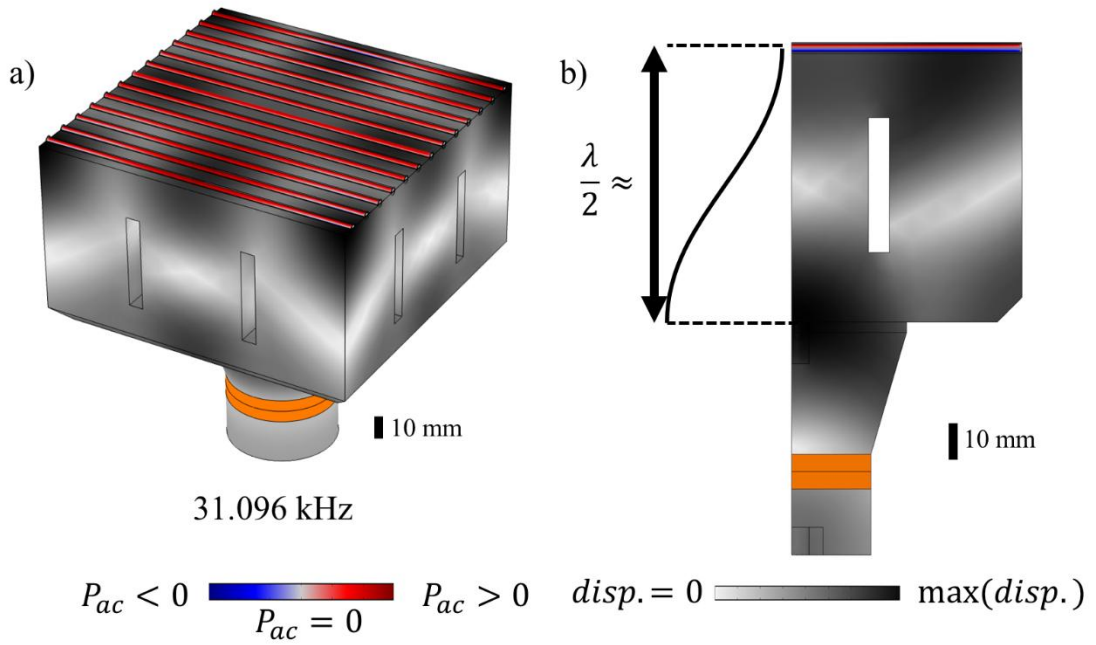

Figure 7. Block-sonotrode (a) showing the expected displacement fields (grey scale) and acoustic pressure (color scale) at the capillary channels. Introducing the slits, the sonotrode acts a multiple waveguide resonating at its half-wavelength across its longitudinal direction (b).

If longer capillary reactors are needed, additional slits can be introduced in block and cylindrical sonotrodes (**Figure 7 and 8,** respectively). These are commonly used in the soldering industry, where the acoustic energy is combined with a hydraulic press to evenly sonicate wider areas [64,84–86]. By introducing slits in the sonotrode, the vibrations propagate as if independent waveguides were used. The enclosed volumes vibrate as independent transducers helping homogenize the displacements at the surface of the sonotrode. The optimized sonotrode designs maintain the ideal distances imposed by half of the wavelength as seen in **Figure 7b and 8b**. The cylindrical sonotrode (**Figure 8**) shows a more homogeneous distribution of the vibrating surface given the axial symmetry and rounded geometry of the assembled device. This can be better appreciated when looking at the vibrational mode of the block sonotrode, where some antinodes are still present at the surface of **Figure 7a**. Again,

attenuation was assumed within the liquid medium to evaluate the acoustic performance in terms of the displacement field. At the scale shown, equal acoustic pressures are obtained for both designs. Although this is not shown in the figures, the reader may foresee the impact of increasing the number of transducers at distinct locations. Acoustic coupling will generate complex vibration modes, which may or may not be in phase, reducing the uniformity in wide vibrating surfaces.

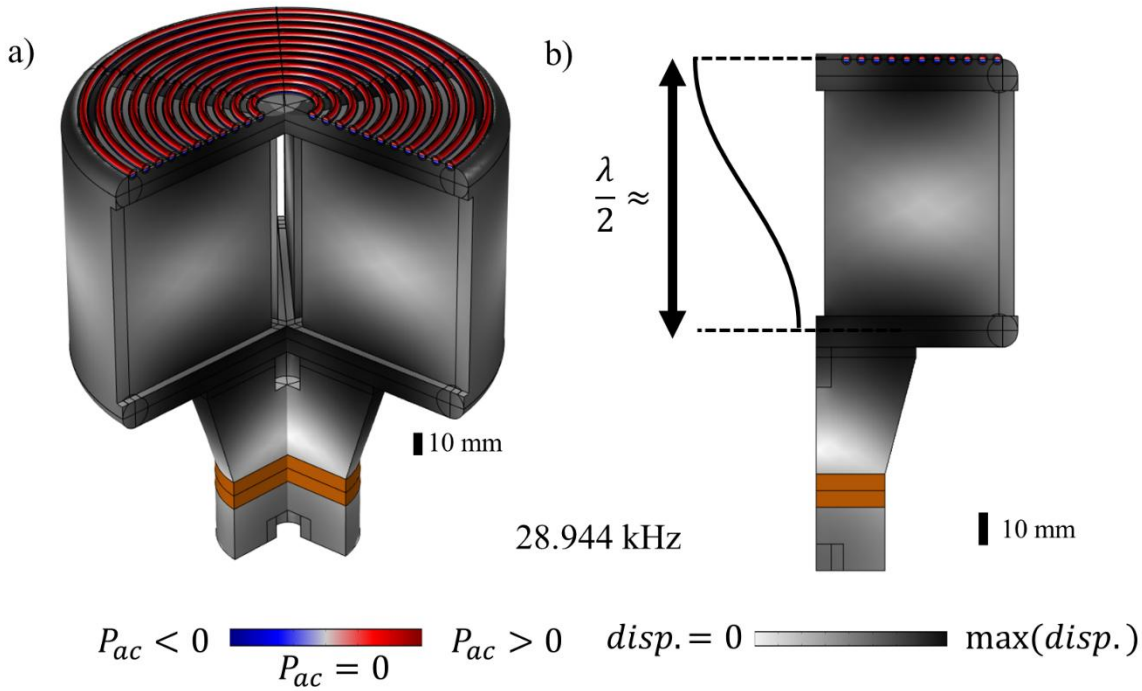

Figure 8. Cylindrical sonotrode with a capillary reactor attached to its emitting surface (a). Axisymmetric designs improve the displacement distribution (grey scale) when combined with slits. The length of the sonotrode corresponds to half of the wavelength (b).

A concentrically stacked sonotrode (**Figure 9**) can be proposed when using piezoelectric rings that are radially polarized [91]. Significantly larger reactor volumes can be achieved with this design by coiling the capillary reactor at the external surface of the sonotrode. Following similar principles as in the traditional wide-block sonoreactors, the use of slits helps homogenize the acoustic field to some extent. Even though for this design a commercial piezo was considered (42-1091 APC International, Ltd. USA), the mechanization and assembly of the concentrically pre-stressed parts might not be trivial.

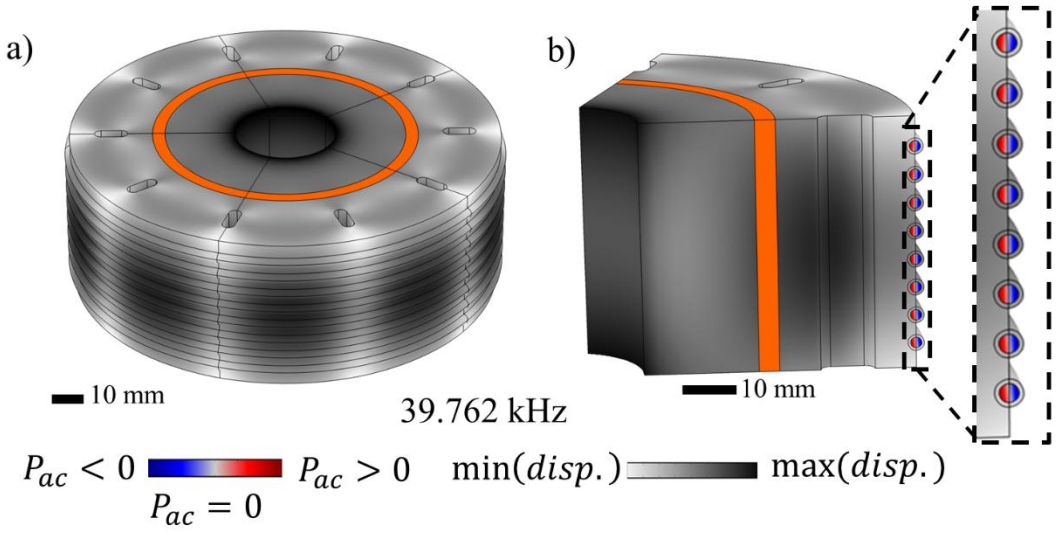

Figure 9. Simulation results of radially polarized piezo tube (42-1091 APC International, Ltd. USA) compromising a back and front parts (a) with slits that help to homogenize the vibration modes. Acoustic pressure is consistently obtained along the 1.58 mm OD reactor tubing (color scale in b) that coils around the cylinder.

The benefits of using commonly available, high-power, low-frequency ultrasonic transducers were further explored. Tapered or cylindrical sonotrodes lead to the appearance of nodes (see Supporting Information), which are a function of the material geometry and the frequency of the transducer. Moreover, as vibrations are mainly longitudinal, there will be a peristaltic pressure difference matching the nodes and antinodes of the sonotrode (a coiled capillary reactor is shown **Figure 10a**). In the literature, helicoidal slits in a sonotrode have been successfully used to transform longitudinal modes into radial and torsional modes [30,92] — traditionally only focused on the benefits obtained at the region close to the tip of the sonotrode [53,93]—. Generalizing this concept of combining different vibrational modes (radial, torsional and longitudinal), a helicoidal capillary reactor was prototyped and built (**Figure 10b**). The simulation results match the experimental observations showing an increase in average amplitude and homogenization of the displacement field (**Figure 10b and 10c**).

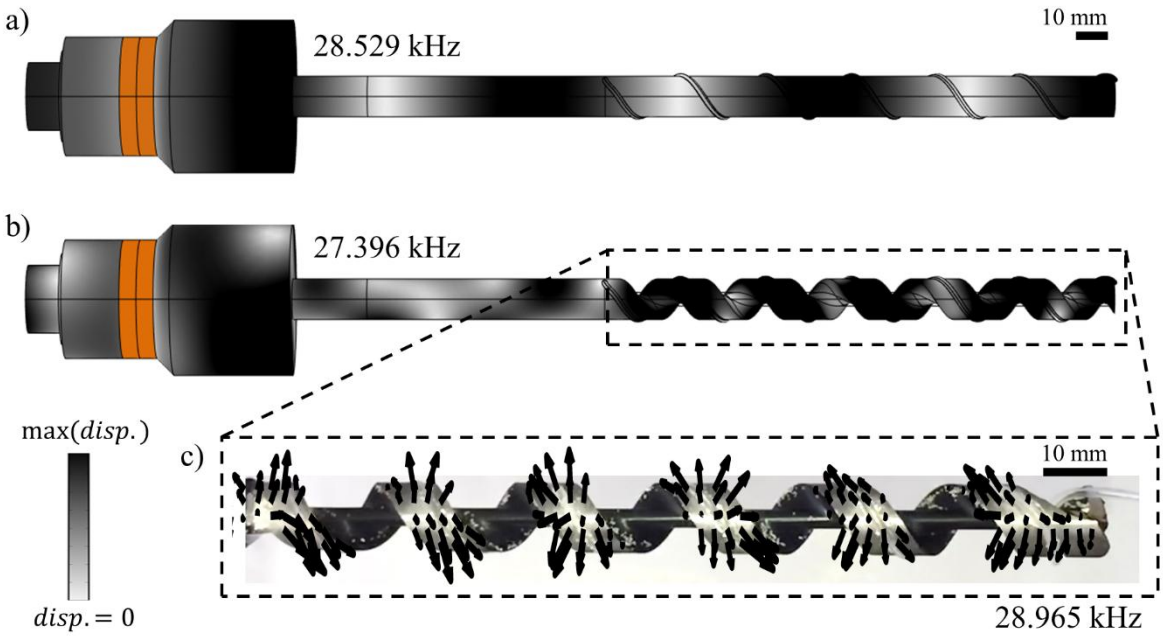

Figure 10. Comparison between the displacement fields of cylindrical- and helicoidal-shaped sonotrodes attached to a commercial 28 kHz ultrasonic power transducer (90-4040 APC International, Ltd. USA). A commercial drill bit (12 mm of diameter and 160 mm of length, BM12x230 Celesa Bluemaster, Spain) was mechanized to admit a 1.58 mm OD of PFA commercial tubing. The vibrational modes of the device were validated against the simulation results (c) showing distributed nodes and antinodes.

The proposed design uses a commercial drill bit as continuous helicoidal waveguide that distributes the standing wave patterns created along the sonotrode (**Figure 10a** compared to **10b**). The displacement field distribution in the helicoidal design was experimentally characterized (**Figure 10c**). Even with low-frequency ultrasound (28 kHz), the spatial performance is improved by reducing longitudinal nodes. The helicoidal sonotrode transforms longitudinal modes into radial and torsional ones, homogenizing the displacement field. The outermost area was used to place a 1.58 mm outer diameter (OD) reactor tubing in a coil threaded manner. The transmission of acoustic energy in the prototyped reactor is solid-to-solid, increasing the sonication efficiency. Different capillary materials, diameters and lengths can be used as well.

A capillary reactor with a continuous vibrating surface can enable chemistry at high concentration of particles. A low-power ultrasound was shown to fluidize a set of particles that were previously forming a clog (**Figure 2**). With the helicoidal capillary sonoreactor, these benefits are no longer confined to regions near sonotrode tips. The scale-up of capillary sonoreactors using longer capillary tubing is now an option. For example, the proposed

helicoidal design was validated using another drill bit with 370 mm instead of 160 mm of total sonotrode length. When injecting 200 μm stainless-steel beads in the capillary tubing coiled along the drill bit, acoustic agitation was observed superimposed with the flow of particles (see supplementary videos).

The acoustic benefits and limitations of the prototypes proposed here will define the next steps of this research. In any case, an early comparison can be made with the computational designs of this work. As illustrated in the figures above, the amplitude and homogeneity of vibration mainly depend on the cross-sectional area reduction and symmetry of the sonotrode, respectively. In this regard, the blade design amplifies the vibration while the axi-symmetric designs yield sharper surface displacement distributions (**Figure 11)**.

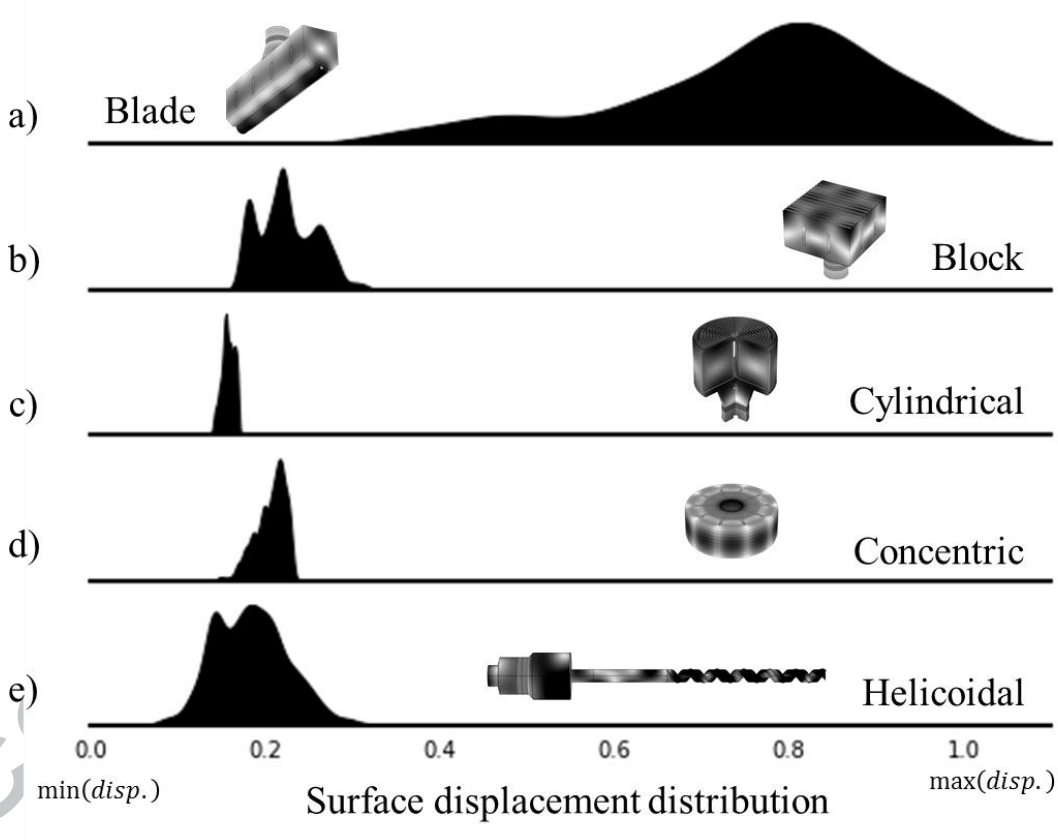

Figure 11. Normalized distribution (kernel density) of the vibrating surface displacements for each design maintaining the electric potential constant. The vibration of the sonotrode increases in amplitude with a decrease of cross-sectional area (a) while its symmetry impacts the sharpness of the distribution (b compared to c and d). The prototyped helicoidal design (e) homogeneously distributes the vibration even when the sonotrode was not optimized as it was built with pre-manufactured parts.

The practicality of scale-up is more difficult to assess at this stage of research (see **Table 1** for a comparison of dimensions). If large volumes but short distances are needed, the blade design would provide a good compromise. If larger reactor lengths are necessary, the concentric sonotrode will provide the most compact design. The helicoidal geometry can also benefit from a sonotrode diameter increase as well as of secondary turns that will reduce its footprint. Overall, the high surface areas per reactor volume (**Table 1**) and the direct contact of the tubing with the sonotrodes can enable simple temperature control solutions for low power ultrasound applications. If the acoustic power is raised to normal operation conditions (20-50W of load power), external fans or cooling fluid circuits will be necessary to control potential temperature increases due to mechanic and electric losses as well as cavitation.

Table 1. Overall dimensions of the different sonotrode designs

	Reactor volume [ml]	Surface area [cm^2]	Length [cm]	Depth [cm]	Height [cm]
Blade	9.78	174.94	30.70	6.96	7.57
Block	6.26	174.63	13.20	13.23	7.87
Cylindrical	8.81	139.70	13.34	13.34	8.63
Concentric	1.58	65.12	6.91	6.91	3.00
Helicoidal	0.24	35.90	15	1.2	1.2

The concept of scaling up for all the designs, except for the blade sonotrode, has been evaluated while maintaining constant the characteristic hydrodynamic length scale of the capillary and only varying its length. The effect of acoustic attenuation when using wider channel sizes, thicker tubing walls, different fluids, construction materials or larger particle sizes require further work and consideration. In any case, we have experimentally covered challenging conditions where the inner diameter is constricted and clogs of microparticles are likely to be formed. Experimental tests involving the precipitation of products or by-products as seen recently in the literature [25] will be the subject of future research.

Recent studies [94] have shown the counterintuitive idea of adding crystals as seeds to a solid forming reaction can increase reactor lifetime, by shifting the solid formation profile from uncontrolled crystal nucleation, to controlled crystal growth. Strategies like this, which harness the generation of a solid by-product, can be utilized along with the sonication technologies presented here to increase continuous flow reactor lifetime.

Conclusions

The proper acoustic design and optimization of sonoreactors have been addressed via numerical simulations. For low-frequency ultrasound and high-power applications, the design of sonotrodes can be limited by the wavelength and uncontrolled resonant modes. When wider sonication areas are necessary, three common sonotrode geometries can be considered: namely, the blade-, block- and cylindrical-type resonator. The acoustic optimization of these sonotrodes for a commercial 28 kHz ultrasonic transducer unveils the importance of limiting their dimension to a quarter of the resonant wavelength, approximatively.

Surfaces vibrating with a low amplitude were shown to effectively stir and unclog particles within a capillary reactor. Cavitation bubbles were not observed at the low voltage applied and therefore this mechanism is not critical to fluidize the clog. This observation is connected to those in granular materials —i.e. arch or bridge formation and their stability under vibrations—. The high-speed microscopic imaging inspired the acoustic design of sonoreactors with wide-output cross-sectional areas.

The introduction of slits improves the uniformity of vibrations and acoustic pressure within capillary sonoreactors. The acoustic design principles shown in this work are necessary to understand the influence of the frequency and sonotrode geometry to control the sonoreactor performance. As an example of this understanding, a novel helicoidal capillary sonoreactor has been proposed and prototyped. Fittings and connectors, prone to clog, can also be firmly attached to the sonotrode.

Helicoidal-shaped capillary sonoreactors can enable the operation of either low-power ultrasound applications (only mechanical benefits such as unclogging removal by vibratory action) or, eventually, high-power ones (cavitation and sonochemistry benefits). In this regard, further experimental studies are under way, including a comparison with ultrasonic baths. In addition, future evaluation of scalable sonotrodes for solid handling should examine the effects of crystal formation, loading and size on the attenuation of acoustic waves as well as their ability to maintain fluidization and prevent clogging.

Acknowledgments.

This research was partially funded by the EU project MAPSYN (Microwave, Acoustic and Plasma SYNtheses) developed in the group of Photochemistry and Electrochemistry of Semiconductors (GFES) at the University of Alicante (Spain), under grant agreement No. CP-IP 309376 of the European Union Seventh Framework Program. Prototyping and experimental costs of the clogging and unclogging visualizations were covered by the Novartis-MIT Centre for Continuous Manufacturing. These initial findings motivated the exploration of scale-up acoustic designs and were performed in collaboration with the Jensen Research Group (MIT, USA). The authors want to thank the MIT Edgerton Center for their technical support as well.

Appendix A. Supplementary data

References

[1] J. Wegner, S. Ceylan, A. Kirschning, Ten key issues in modern flow chemistry., Chem. Commun. (Camb). 47 (2011) 4583–92. doi:10.1039/c0cc05060a.

[2] J. Zhang, K. Wang, A.R. Teixeira, K.F. Jensen, G. Luo, Design and Scaling Up of Microchemical Systems: A Review, Annu. Rev. Chem. Biomol. Eng. 8 (2017) 285–305. doi:10.1146/annurev-chembioeng-060816-101443.

[3] A. Adamo, R.L. Beingessner, M. Behnam, J. Chen, T.F. Jamison, K.F. Jensen, J.-C.M. Monbaliu, A.S. Myerson, E.M. Revalor, D.R. Snead, T. Stelzer, N. Weeranoppanant, S.Y. Wong, P. Zhang, On-demand continuous-flow production of pharmaceuticals in a compact, reconfigurable system, Science (80-.). 352 (2016) 61–67. doi:10.1126/science.aaf1337.

[4] K. Wu, S. Kuhn, Strategies for solids handling in microreactors, Chim. Oggi. 32 (2014) 62–66.

[5] F. Scheiff, D.W. Agar, Solid Particle Handling in Microreaction Technology: Practical Challenges and Application of Microfluid Segments for Particle-Based Processes, in: J.M. Köhler, B.P. Cahill (Eds.), Micro-Segmented Flow Appl. Chem. Biol., Springer Berlin Heidelberg, Berlin, Heidelberg, 2014: pp. 103–148. doi:10.1007/978-3-642-38780-7_6.

[6] Y. Chen, J.C. Sabio, R.L. Hartman, When Solids Stop Flow Chemistry in Commercial Tubing, 5 (2015) 166–171. doi:10.1556/1846.2015.00001.

[7] H. Wang, A. Mustaffar, A.N. Phan, V. Zivkovic, D. Reay, R. Law, K. Boodhoo, A review of process intensification applied to solids handling, Chem. Eng. Process. Process Intensif. 118 (2017) 78–107. doi:https://doi.org/10.1016/j.cep.2017.04.007.

[8] S. Kuhn, T. Noël, L. Gu, P.L. Heider, K.F. Jensen, A Teflon microreactor with integrated piezoelectric actuator to handle solid forming reactions., Lab Chip. 11 (2011) 2488–92. doi:10.1039/c1lc20337a.

[9] B.S. Flowers, R.L. Hartman, Particle Handling Techniques in Microchemical Processes, Challenges. 3 (2012) 194–211. doi:10.3390/challe3020194.

[10] F.. Castro, S.. Kuhn, K.. Jensen, A.. Ferreira, F.. Rocha, A.. Vicente, J.A.. Teixeira, Continuous-flow precipitation of hydroxyapatite in ultrasonic microsystems, Chem. Eng. J. 215–216 (2013) 979–987. doi:https://doi.org/10.1016/j.cej.2012.11.014.

[11] D. Fernandez Rivas, S. Kuhn, Synergy of Microfluidics and Ultrasound: Process Intensification Challenges and Opportunities, Top. Curr. Chem. 374 (2016) 70. doi:10.1007/s41061-016-0070-y.

[12] D. Fernandez Rivas, P. Cintas, H.J.G.E. Gardeniers, Merging microfluidics and sonochemistry: towards greener and more efficient micro-sono-reactors., Chem. Commun. (Cambridge, U. K.). 48 (2012) 10935–10947. doi:10.1039/c2cc33920j.

[13] D.F. Rivas, S. Kuhn, Synergy of Microfluidics and Ultrasound, Top. Curr. Chem. 374 (2016) 1–30. doi:10.1007/s41061-016-0070-y.

[14] D. Zhengya, Z. Shuainan, Z. Yuchao, Y. Chaoqun, Y. Quan, C. Guangwen, Mixing and residence time distribution in ultrasonic microreactors, AIChE J. 63 (2016) 1404–1418.

[15] S. Hübner, S. Kressirer, D. Kralisch, C. Bludszuweit-Philipp, K. Lukow, I. Jänich, A. Schilling, H. Hieronymus, C. Liebner, K. Jähnisch, Ultrasound and Microstructures—A Promising Combination?, ChemSusChem. 5 (2012) 279–288. doi:10.1002/cssc.201100369.

[16] P. Cintas, G. Palmisano, G. Cravotto, Power ultrasound in metal-assisted synthesis: From classical Barbier-like reactions to click chemistry, Ultrason. Sonochem. 18 (2011) 836–841. doi:10.1016/J.ULTSONCH.2010.11.020.

[17] P. Cintas, S. Tagliapietra, M. Caporaso, S. Tabasso, G. Cravotto, Enabling technologies built on a sonochemical platform: Challenges and opportunities, Ultrason. Sonochem. 25 (2015) 8–16. doi:10.1016/J.ULTSONCH.2014.12.004.

[18] G. Cravotto, L. Boffa, S. Mantegna, P. Perego, M. Avogadro, P. Cintas, Improved extraction of vegetable oils under high-intensity ultrasound and/or microwaves., Ultrason. Sonochem. 15 (2008) 898–902. doi:10.1016/j.ultsonch.2007.10.009.

[19] S. Aljbour, H. Yamada, T. Tagawa, Ultrasound-assisted phase transfer catalysis in a capillary microreactor, Chem. Eng. Process. Process Intensif. 48 (2009) 1167–1172. doi:10.1016/j.cep.2009.04.004.

[20] Tandiono, S.-W. Ohl, D.S.-W. Ow, E. Klaseboer, V.V.T. Wong, A. Camattari, C.-D. Ohl, Creation of cavitation activity in a microfluidic device through acoustically driven capillary waves., Lab Chip. 10 (2010) 1848–55. doi:10.1039/c002363a.

[21] D. Rossi, R. Jamshidi, N. Saffari, S. Kuhn, A. Gavriilidis, L. Mazzei, Continuous-Flow Sonocrystallization in Droplet-Based Microfluidics, Cryst. Growth Des. 15 (2015) 5519–5529. doi:10.1021/acs.cgd.5b01153.

[22] Y. Iida, K. Yasui, T. Tuziuti, M. Sivakumar, Y. Endo, Ultrasonic cavitation in microspace, Chem. Commun. (2004) 2280. doi:10.1039/b410015h.

[23] P. Glynne-Jones, R.J. Boltryk, M. Hill, Chapter 7 Modelling and Applications of Planar Resonant Devices for Acoustic Particle Manipulation, in: Microscale Acoustofluidics,

The Royal Society of Chemistry, 2015: pp. 127–147. doi:10.1039/9781849737067-00127.

[24] J. Dual, D. Möller, Piezoelectricity and Application to the Excitation of Acoustic Fields for Ultrasonic Particle Manipulation, in: Microscale Acoustofluidics, The Royal Society of Chemistry, 2015: pp. 81–99. doi:10.1039/9781849737067-00081.

[25] Z. Dong, D. Fernandez Rivas, S. Kuhn, Acoustophoretic focusing effects on particle synthesis and clogging in microreactors, Lab Chip. 19 (2019) 316–327. doi:10.1039/C8LC00675J.

[26] Guidelines for the design of efficient sono-microreactors , Green Process. Synth. . 3 (2014) 311. doi:10.1515/gps-2014-0052.

[27] H. Minchenko, High-Power Piezoelectric Transducer Design, IEEE Trans. Sonics Ultrason. 16 (1969) 126–131. doi:10.1109/T-SU.1969.29514.

[28] S. Sherrit, B.P. Dolgin, Y. Bar-Cohen, D. Pal, J. Kroh, T. Peterson, Modeling of horns for sonic/ultrasonic applications, in: 1999 IEEE Ultrason. Symp. Proceedings. Int. Symp. (Cat. No.99CH37027), 1999: pp. 647–651 vol.1. doi:10.1109/ULTSYM.1999.849482.

[29] S. Sherrit, S.P. Leary, B.P. Dolgin, Y. Bar-Cohen, Comparison of the Mason and KLM equivalent circuits for piezoelectric resonators in the thickness mode, 1999 IEEE Ultrason. Symp. Proceedings. Int. Symp. (Cat. No.99CH37027). 2 (1999) 921–926. doi:10.1109/ULTSYM.1999.849139.

[30] H. Al-Budairi, M. Lucas, P. Harkness, A design approach for longitudinal–torsional ultrasonic transducers, Sensors Actuators A Phys. 198 (2013) 99–106. doi:10.1016/j.sna.2013.04.024.

[31] L. de los S. Castillo-Peinado, M.D. Castro de Luque, The role of ultrasound in pharmaceutical production: sonocrystallization, J. Pharm. Pharmacol. 68 (2016) 1249–1267.

[32] J. Wang, F. Li, R. Lakerveld, Process intensification for pharmaceutical crystallization, Chem. Eng. Process. - Process Intensif. 127 (2018) 111–126. doi:https://doi.org/10.1016/j.cep.2018.03.018.

[33] P. Cintas, S. Mantegna, E.C. Gaudino, G. Cravotto, A new pilot flow reactor for high-intensity ultrasound irradiation. Application to the synthesis of biodiesel, Ultrason. Sonochem. 17 (2010) 985–989. doi:10.1016/J.ULTSONCH.2009.12.003.

[34] P.R. Gogate, V.S. Sutkar, A.B. Pandit, Sonochemical reactors: Important design and scale up considerations with a special emphasis on heterogeneous systems, Chem. Eng. J. 166 (2011) 1066–1082. doi:10.1016/j.cej.2010.11.069.

[35] P.R. Gogate, A.B. Pandit, Design and scale-up of sonochemical reactors for food processing and other applications, Elsevier Ltd., 2014. doi:10.1016/B978-1-78242-028-6.00024-7.

[36] M.B. Plutschack, B. Pieber, K. Gilmore, P.H. Seeberger, The Hitchhiker's Guide to Flow Chemistry, Chem. Rev. 117 (2017) 11796–11893. doi:10.1021/acs.chemrev.7b00183.

[37] T. Noel, J.R. Naber, R.L. Hartman, J.P. McMullen, K.F. Jensen, S.L. Buchwald, Palladium-catalyzed amination reactions in flow: overcoming the challenges of clogging via acoustic irradiation, Chem. Sci. 2 (2011) 287–290. doi:10.1039/C0SC00524J.

[38] R.L. Hartman, Managing Solids in Microreactors for the Upstream Continuous

Processing of Fine Chemicals, (2012).

[39] D. Fernandez Rivas, L. Stricker, A.G. Zijlstra, H.J.G.E. Gardeniers, D. Lohse, A. Prosperetti, Ultrasound artificially nucleated bubbles and their sonochemical radical production, Ultrason. Sonochem. 20 (2013) 510–524. doi:10.1016/J.ULTSONCH.2012.07.024.

[40] D.F. Rivas, B. Verhaagen, Preface to the Special Issue: Cleaning with bubbles, Ultrason. Sonochem. 29 (2016) 517–518. doi:10.1016/J.ULTSONCH.2015.11.012.

[41] T.J. Mason, Ultrasonic cleaning: An historical perspective, Ultrason. Sonochem. 29 (2016) 519–523. doi:10.1016/J.ULTSONCH.2015.05.004.

[42] T.J. Bulat, Macrosonics in industry: 3. Ultrasonic cleaning, Ultrasonics. 12 (1974) 59–68. doi:10.1016/0041-624X(74)90032-8.

[43] D.H. McQueen, Frequency dependence of ultrasonic cleaning, Ultrasonics. 24 (1986) 273–280. doi:10.1016/0041-624X(86)90105-8.

[44] F. Gomes, H. Thakkar, A. Lähde, B. Verhaagen, A.B. Pandit, D. Fernández Rivas, Is reproducibility inside the bag? Special issue fundamentals and applications of sonochemistry ESS-15, Ultrason. Sonochem. 40 (2018) 163–174. doi:10.1016/J.ULTSONCH.2017.03.037.

[45] F.J. Navarro-Brull, A.R. Teixeira, J. Zhang, R. Gómez, K.F. Jensen, Reduction of Dispersion in Ultrasonically-Enhanced Micropacked Beds, Ind. Eng. Chem. Res. 57 (2018) 122–128. doi:10.1021/acs.iecr.7b03876.

[46] C. Lozano, I. Zuriguel, A. Garcimartín, Stability of clogging arches in a silo submitted to vertical vibrations., Phys. Rev. E. Stat. Nonlin. Soft Matter Phys. 91 (2015) 62203. doi:10.1103/PhysRevE.91.062203.

[47] B. Guerrero, C. Lozano, I. Zuriguel, A. Garcimartín, Dynamics of breaking arches under a constant vibration, EPJ Web Conf. 140 (2017) 3016. doi:10.1051/epjconf/201714003016.

[48] I. Zuriguel, Á. Janda, R. Arévalo, D. Maza, Á. Garcimartín, Clogging and unclogging of many-particle systems passing through a bottleneck, EPJ Web Conf. 140 (2017) 1002. doi:10.1051/epjconf/201714001002.

[49] D. Bi, J. Zhang, B. Chakraborty, R.P. Behringer, Jamming by shear, Nature. 480 (2011) 355.

[50] A. Ashour, S. Wegner, T. Trittel, T. Börzsönyi, R. Stannarius, Outflow and clogging of shape-anisotropic grains in hoppers with small apertures, Soft Matter. 13 (2017) 402–414. doi:10.1039/C6SM02374F.

[51] F. Radjai, Modeling force transmission in granular materials, Comptes Rendus Phys. 16 (2015) 3–9. doi:https://doi.org/10.1016/j.crhy.2015.01.003.

[52] R. Blanco-Rodriguez, G. Perez-Angel, Stress distribution in two-dimensional silos, Phys. Rev. E. 97 (2018) 12903. doi:10.1103/PhysRevE.97.012903.

[53] M. Lucas, A. Mathieson, Ultrasonic cutting for surgical applications, Elsevier Ltd., 2014. doi:10.1016/B978-1-78242-028-6.00023-5.

[54] E.A. Neppiras, Macrosonics in industry 1. Introduction, Ultrasonics. 10 (1972) 9–13. doi:10.1016/0041-624X(72)90207-7.

[55] G. Harvey, A. Gachagan, T. Mutasa, Review of high-power ultrasound-industrial

applications and measurement methods, IEEE Trans. Ultrason. Ferroelectr. Freq. Control. 61 (2014) 481–495. doi:10.1109/TUFFC.2014.2932.

[56] J.A. Gallego-Juárez, G. Rodríguez, V.M. Acosta-Aparicio, E. Riera, A. Cardoni, 7 - Power ultrasonic transducers with vibrating plate radiators*, 2015. doi:http://dx.doi.org/10.1016/B978-1-78242-028-6.00007-7.

[57] J.A. Gallego-Juárez, K.F. Graff, Introduction to power ultrasonics, Power Ultrason. Appl. High-Intensity Ultrasound. (2014) 1–6. doi:10.1016/B978-1-78242-028-6.00001-6.

[58] E.A. Neppiras, The pre-stressed piezoelectric sandwich transducer, Ultrason. Int. Conf. Proc. (1973) 295–301.

[59] J.A. Gallego-Juarez, Piezoelectric ceramics and ultrasonic transducers, J. Phys. E. 22 (1989) 804.

[60] L. Shuyu, Z. Fucheng, Study of vibrational characteristics for piezoelectric sandwich ultrasonic transducers, Ultrason. 32 (1994) 39–42. doi:http://dx.doi.org/10.1016/0041-624X(94)90078-7.

[61] K.F. Graff, Power ultrasonic transducers: principles and design, in: J.A. Gallego-Juárez, K.F. Graff (Eds.), Power Ultrason., Woodhead Publishing, Oxford, 2015: pp. 127–158. doi:https://doi.org/10.1016/B978-1-78242-028-6.00006-5.

[62] T.J. Mason, J.P. Lorimer, Applied Sonochemistry: Uses of Power Ultrasound in Chemistry and Processing, Wiley-VCH Verlag GmbH & Co. KGaA, 2003. doi:10.1002/352760054X.

[63] A. Mathieson, A. Cardoni, N. Cerisola, M. Lucas, The influence of piezoceramic stack location on nonlinear behavior of langevin transducers, IEEE Trans. Ultrason. Ferroelectr. Freq. Control. 60 (2013) 1126–1133. doi:10.1109/TUFFC.2013.2675.

[64] P.L.L.M. Derks, The design of ultrasonic resonators with wide output cross-sections, Technische Hogeschool Eindhoven, 1984. doi:10.6100/IR34306.

[65] D. Ensminger, F.B. Stulen, Ultrasonics: Data, Equations and Their Practical Uses, CRC Press, Boca Raton, 2008.

[66] a Mathieson, a Cardoni, N. Cerisola, M. Lucas, The influence of piezoceramic stack location on nonlinear behavior of langevin transducers., IEEE Trans. Ultrason. Ferroelectr. Freq. Control. 60 (2013) 1126–33. doi:10.1109/TUFFC.2013.2675.

[67] O. Louisnard, J. Gonzalez-Garcia, I. Tudela, J. Klima, V. Saez, Y. Vargas-Hernandez, FEM simulation of a sono-reactor accounting for vibrations of the boundaries., Ultrason. Sonochem. 16 (2009) 250–259.

[68] I. Tudela, V. Sáez, M.D. Esclapez, P. Bonete, H. Harzali, F. Baillon, J. González-García, O. Louisnard, Study of the influence of transducer-electrode and electrode-wall gaps on the acoustic field inside a sonoelectrochemical reactor by FEM simulations, Chem. Eng. J. 171 (2011) 81–91. doi:10.1016/j.cej.2011.03.064.

[69] J. Dual, P. Hahn, I. Leibacher, D. Möller, T. Schwarz, Acoustofluidics 6: Experimental characterization of ultrasonic particle manipulation devices., Lab Chip. 12 (2012) 852–62. doi:10.1039/c2lc21067c.

[70] J. Dual, P. Hahn, I. Leibacher, D. Möller, T. Schwarz, J. Wang, Acoustofluidics 19: Ultrasonic microrobotics in cavities: devices and numerical simulation, Lab Chip. 12 (2012) 4010–4021. doi:10.1039/C2LC40733G.

[71] I. Tudela, V. Sáez, M.D. Esclapez, M.I. D'iez-Garc'ia, P. Bonete, J. González-Garc'ia, Simulation of the spatial distribution of the acoustic pressure in sonochemical reactors with numerical methods: A review, Ultrason. Sonochem. 21 (2014) 909–919. doi:10.1016/j.ultsonch.2013.11.012.

[72] P. Hahn, O. Schwab, J. Dual, Modeling and optimization of acoustofluidic micro-devices, Lab Chip. 14 (2014) 3937–3948. doi:10.1039/C4LC00714J.

[73] P. Hahn, J. Dual, A numerically efficient damping model for acoustic resonances in microfluidic cavities, Phys. Fluids. 27 (2015) 62005. doi:10.1063/1.4922986.

[74] F.J. Navarro-Brull, P. Poveda, R. Ruiz-Femenia, P. Bonete, J. Ramis, R. Gómez, Guidelines for the design of efficient sono-microreactors, Green Process. Synth. 3 (2014) 311–320. doi:10.1515/gps-2014-0052.

[75] O.A. Sapozhnikov, High-intensity ultrasonic waves in fluids: Nonlinear propagation and effects, Elsevier Ltd., 2014. doi:10.1016/B978-1-78242-028-6.00002-8.

[76] A. Alippi, High-intensity ultrasonic waves in solids: nonlinear dynamics and effects, in: J.A. Gallego-Juárez, K.F.B.T.-P.U. Graff (Eds.), Power Ultrason., Woodhead Publishing, Oxford, 2015: pp. 79–99. doi:https://doi.org/10.1016/B978-1-78242-028-6.00004-1.

[77] B. Ducharne, D. Guyomar, G. Sébald, B. Zhang, Modeling energy losses in power ultrasound transducers, in: J.A. Gallego-Juárez, K.F.B.T.-P.U. Graff (Eds.), Power Ultrason., Woodhead Publishing, Oxford, 2015: pp. 241–256. doi:https://doi.org/10.1016/B978-1-78242-028-6.00010-7.

[78] O. Louisnard, A simple model of ultrasound propagation in a cavitating liquid. Part I: Theory, nonlinear attenuation and traveling wave generation., Ultrason. Sonochem. 19 (2012) 56–65. doi:10.1016/j.ultsonch.2011.06.007.

[79] O. Louisnard, A simple model of ultrasound propagation in a cavitating liquid. Part II: Primary Bjerknes force and bubble structures., Ultrason. Sonochem. 19 (2012) 66–76. doi:10.1016/j.ultsonch.2011.06.008.

[80] O. Louisnard, A viable method to predict acoustic streaming in presence of cavitation, Ultrason. Sonochem. 35 (2017) 518–524. doi:https://doi.org/10.1016/j.ultsonch.2016.09.013.

[81] J. Zhang, A.R. Teixeira, L.T. Kögl, L. Yang, K.F. Jensen, Hydrodynamics of Gas-Liquid Flow in Micro-Packed Beds: Pressure Drop, Liquid Holdup and Two-Phase Model, AIChE J. (2017). doi:10.1002/aic.15807.

[82] J. Zhang, A. Teixeira, Jensen. Klavs F., Automated measurements of gas-liquid mass transfer in micropacked bed reactors, AIChE J. 64 (2017) 564–570.

[83] W. Thielicke, E.J. Stamhuis, PIVlab – Towards User-friendly, Affordable and Accurate Digital Particle Image Velocimetry in MATLAB, J. Open Res. Softw. 2 (2014) e30. doi:http://doi.org/10.5334/jors.bl.

[84] M.P. Matheny, K.F. Graff, Ultrasonic welding of metals, Elsevier Ltd., 2014. doi:10.1016/B978-1-78242-028-6.00011-9.

[85] A. Benatar, Ultrasonic welding of plastics and polymeric composites, Elsevier Ltd., 2014. doi:10.1016/B978-1-78242-028-6.00012-0.

[86] M. Short, K.F. Graff, 16 - Using power ultrasonics in machine tools, Elsevier Ltd., 2015. doi:10.1016/B978-1-78242-028-6.00016-8.

[87] J.J. John, S. Kuhn, L. Braeken, T. Van Gerven, Temperature controlled interval contact design for ultrasound assisted liquid–liquid extraction, Chem. Eng. Res. Des. 125 (2017) 146–155. doi:https://doi.org/10.1016/j.cherd.2017.06.025.

[88] J. Wang, B. Liu, G. Kan, G. Li, J. Zheng, X. Meng, Frequency dependence of sound speed and attenuation in fine-grained sediments from 25 to 250 kHz based on a probe method, Ocean Eng. 160 (2018) 45–53. doi:10.1016/J.OCEANENG.2018.04.078.

[89] J.P. Sessarego, R. Guillermin, High-frequency sound-speed, attenuation, and reflection measurements using water-saturated glass beads of different sizes, IEEE J. Ocean. Eng. 37 (2012) 507–515. doi:10.1109/JOE.2012.2194410.

[90] K.L. Williams, D.R. Jackson, E.I. Thorsos, D. Tang, S.G. Schock, Comparison of sound speed and attenuation measured in a sandy sediment to predictions based on the Biot theory of porous media, IEEE J. Ocean. Eng. 27 (2002) 413–428. doi:10.1109/JOE.2002.1040928.

[91] J. Xu, S. Lin, Y. Ma, Y. Tang, Analysis on Coupled Vibration of a Radially Polarized Piezoelectric Cylindrical Transducer, Sensors (Basel). 17 (2017) 2850. doi:10.3390/s17122850.

[92] Z. Long, Y. Liu, Z. Zhang, S. Liu, J. Zhou, Design for torsional transducer in ultrasonic machining based on equivalent circuit, in: 2017 IEEE Int. Conf. Inf. Autom., 2017: pp. 953–958. doi:10.1109/ICInfA.2017.8079040.

[93] M.E. Schafer, 21 - Ultrasonic surgical devices and procedures, Elsevier Ltd., 2015. doi:http://dx.doi.org/10.1016/B978-1-78242-028-6.00021-1.

[94] G. Giri, L. Yang, Y. Mo, K.F. Jensen, Adding Crystals To Minimize Clogging in Continuous Flow Synthesis, Cryst. Growth Des. 19 (2019) 98–105. doi:10.1021/acs.cgd.8b00999.

HIGHLIGHTS

- Low power US effectively used for preventing and removing clogging in capillaries
- Computer-aided prototyping of sonoreactors with wider and uniform sonication areas
- Limitations of blade, block and cylindrical sonotrodes using slits are highlighted
- Novel helicoidal design for accommodating longer capillary sonoreactors